Proceedings of The Canadian Society for Mechanical Engineering International Congress 2018
CSME International Congress 2018
May 27-30, 2018, Toronto, On, Canada

MODELLING THERMAL CONDUCTIVITY OF POROUS THERMAL BARRIER COATINGS FOR HIGH-TEMPERATURE AERO ENGINES USING FIVE PHASE MODEL

Ramandeep Singh Ghai
Department of Mechanical Engineering
University of Ottawa
Ottawa, Canada
rghai036@uottawa.ca

Dr. Kuiying Chen
Aerospace Portfolio
National Research Council Canada
Ottawa, Canada

Dr. Natalie Baddour
Department of Mechanical Engineering
University of Ottawa
Ottawa, Canada

Abstract**—** Thermal Barrier Coatings (TBC) are used to shield hot sections of gas turbine engines, helping to prevent the melting of metallic surfaces. This paper proposes a Five-phase model to calculate the effective thermal conductivity of a TBC, taking into consideration the effect of various defects. By comparing the predicted values with experimental results, it was shown that the proposed five-phase model can predict the thermal conductivity of ceramic coatings closer to the actual values.

Keywords- TBC, Thermal Conductivity, High-temperature coatings, Modelling, Porosity and Defects.

I. INTRODUCTION

The advancement in high-temperature engineering alloys led to the design and development of the present era turbine engines. The laws of thermodynamics suggest that with an increase in inlet operating temperature, the performance and efficiency of an engine can be increased [1].

The components of a turbine engine are exposed to elevated temperatures as well as to an oxidative and corrosive gaseous environment. In certain cases, there are some impacts from high-velocity foreign particles during operation [2]–[4]. The components used at elevated temperatures are coated with a ceramic coating to have protection against high-temperature degradation. A Thermal Barrier Coating (TBC) provides thermal shock resistance, creep resistance, strain tolerance, protection against hot corrosion and stability to the substrate at higher temperatures [5] [6].

The simple structure of the TBC system consists of the ceramic top coat, bond coat and superalloy substrate. During service life, a thermally grown oxide (TGO) layer (mostly α-Al_2O_3) forms on the bond coat surface and reduces the rate of oxidation [7]. The objective of the top ceramic coating is to reduce the metal temperature. A metallic bond coat is used to enhance the bonding between the top coat and the underlying super-alloy and to protect the super-alloy from oxidation and hot corrosion [8]. Yttria-stabilized Zirconia [YSZ] containing 6-8%Y_2O_3 is known as a state of the art thermal barrier coating topcoat [9].

The key properties of YSZ TBC are low thermal conductivity, high melting point, phase compatibility with alpha alumina, and the combination of good resistance to corrosion and damage from large particle impacts [10]. The microstructure of ceramic coatings is highly heterogeneous as it consists of imperfections such as pores, voids, and vacancies, along with cracks of different shapes and sizes. Overall, the thermal conductivity of the coating is highly affected by the presence of such defects [11], [12] and spraying parameters [13]. The extent of change in the thermal and mechanical properties depends on the amount, size, and morphology of the defects present in the coating.

Defects lead to a lower value for thermal conductivity and a lower thermal conductivity implies a longer service life, as heat transfer to the substrate is reduced. Lower heat transfer into the substrate also leads to lower damage to the coating interface, where most of the failure occurs [8]. To achieve lower values for thermal conductivity, better strain tolerance and higher lifetime, the distribution of cracks and pores in the coating needs to be optimized [14]. It thus becomes essential to understand the fundamental microstructural properties of the TBC in order to produce an optimized coating. Hence, one of the aims of TBC design is to design coatings with a lower thermal conductivity. Therefore, modelling provides an economical way to develop and understand the coating microstructure that will have lower thermal conductivity. This paper proposed a five-phase model for calculating the effective thermal conductivity of a TBC with the goal to improve the accuracy of modelling.

II. MODELLING THERMAL CONDUCTIVITY

A. *Modelling approach*

Modelling or/and simulation is a cost-effective and flexible approach to optimize and understand the coating microstructure. Development of new types of coatings design or new structures can easily be performed. Modification of the

---

Special Thanks to Dr. Natalie Baddour for sponsoring this paper.

parameters is simple, and the analysis can be performed quickly compared to a traditional experimental approach. Simulation can provide analysis of different microstructural parameters and their individual effect, as well as the combined effect on the TBC.

The present study is based on the different types of defects (pores, voids and cracks) that are present in the coating during the fabrication of the coating. The effect of various defects needs to be included in the model to better predict the thermal conductivity of coating and to have a better understanding of the coating microstructure. Many researchers have presented models that can predict and calculate the thermal conductivity of the porous coatings. Out of those models, Bruggeman's formula provides a model that takes into consideration the shape, orientation and volumetric fraction of pores. The details can be found in next section.

B. *Two-phase model for thermal conductivity*

Thermal conductivity (*k*), is the measure of heat transfer from one surface to another that is having a cross-sectional area *A* and are separated by a distance *L*. There are many formulas to calculate thermal conductivity depending on the coatings and its parameters. The thermal conductivity of free-standing materials can be determined by [15]

$$k = \alpha C_p \rho \tag{1}$$

where ρ is the density of the free-standing material (kg/m3), C_p indicates the heat capacity of materials at constant pressure (J/(kg K)), and α is the thermal diffusion rate (m^2/s).

Bruggeman provided a model to predict the thermal conductivity of porous coatings [16]. Bruggeman extended the Maxwell model to systems having random dispersions of spherical particles of several sizes. He proposed a model assuming that if a relatively large spherical particle is introduced into a dispersion containing much smaller particles, there will be a negligible disturbance of the field around the large sphere due to the small spheres. With this model, he showed that the limitation on a volumetric fraction of dilute dispersion can be removed. The Maxwell model is extended to [17]

$$\frac{k-k_m}{k+2k_m} = f\,\frac{k_d-k_m}{k_d+2k_m} \tag{2}$$

where k is the thermal conductivity of the composite, k_m is the thermal conductivity of the matrix, k_d is the thermal conductivity of the dispersed phase, and f is the volumetric fraction of the i^{th} phase. A change in conductivity *dM*, with the change in volume fraction of the dispersed phase, is expressed as

$$\frac{dM}{3M} = \frac{dP}{1+P}\left(\frac{k_d-M}{k_d+2M}\right) \tag{3}$$

Integrating P from 0 to $f/(1+f)$ and M from k_m to k. leads to Bruggeman's two-phase model given by

$$\left(\frac{\dfrac{k}{k_m}-\dfrac{k_d}{k_m}}{\left(\dfrac{k}{k_m}\right)^{\frac{1}{3}}\left(1-\dfrac{k_d}{k_m}\right)}\right) = \left(1-f\right) \tag{4}$$

An example for the two-phase coating can be seen in Figure 1. Also, in this case, it is possible to generalise the modelling to a solute dispersion of randomly oriented ellipsoids.

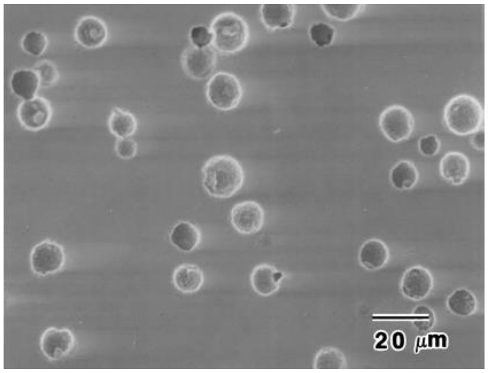

Figure 1 Scanning Electron Microscopic Image of spherical pores in continuous matrix [18]

Some assumptions in this work are as follows:

- The thermal conductivity of the dispersed phase or of the defect is assumed to be negligible.
- Heat transfer is along the thickness of the coating only (or perpendicular to bond coat-substrate interface). No lateral heat transfer is assumed.
- The effect of connected pores is neglected.
- There is a linear relation between the porosity and thermal conductivity.

III. FIVE PHASE MODEL FOR THERMAL CONDUCTIVITY

A. *Simplification of Bruggeman two-phase model*

Bruggeman's model is further simplified by assuming the thermal conductivity of pores/defects is negligible i.e. $k_d = 0$. Under the condition of non-radiating pores, the equation (4) reduces to

$$\frac{k}{k_m} = \left(1-f\right)^{\frac{3}{2}} \tag{5}$$

This equation is the special case when the pores are of spherical shape. The Bruggeman model is based on ellipsoids of revolution, hence in general, for the dispersion of an ellipsoid, the Bruggeman model is a modified version of the equation (5) and is given by [19]

$$\frac{k}{k_m} = \left(1-f\right)^{X} \tag{6}$$

where the value of X depends on certain factors such as the shape factor of the ellipsoid (F) and α, which is the angle between the heat flux and the axis of revolution. The value of X can be described by [19]

$$X = \frac{1-\cos^2\alpha}{1-F} + \frac{\cos^2\alpha}{2F} \tag{7}$$

The value X is set to 3/2 when there are only spherical pores in a continuous matrix. The assumption of non-conducting pores/defects is valid for a certain temperature limit, however, its primary purpose is to simplify the model [16].

In reality, coatings contain several types of defects [11], [20]–[22]. Therefore, for more realistic modelling of coatings, superposition of the contributions of different defects types on the overall thermal conductivity is required. One approach is to iterate the Bruggeman's two-phase model to higher levels of porosities. This approach is explained in detail in subsequent paragraphs.

B. Iteration Approach

This approach works in two steps, first of all, type 1 porosity is added in the continuous matrix so that the average thermal conductivity of a binary mixture is obtained. Then, for the second step, the binary mixture is considered as a continuous matrix, and subsequently, type 2 porosity is added in the same manner. This gives the combination of two different types of porosities in a continuous matrix. Suppose that f_1 and f_2 are the final percentages of type 1 and type 2 porosity, respectively, then the total porosity in the coating is given by f, which is given as the sum of the different types of porosities. Therefore, $f = f_1 + f_2$. There can be two ways of adding the defects in a continuous matrix. Consider if we add a Type 1 porosity first into the continuous matrix and then add a Type 2 porosity. This will lead to an equation given by

$$\left\{ \Phi\left[\frac{f_2}{1-f_1}\right]\Psi\left(f_1\right) \right\} \tag{8}$$

Now consider if we first add Type 2 porosity in the continuous matrix and then Type 1, this will generate the formula as-

$$\left\{ \Psi\left[\frac{f_1}{1-f_2}\right]\Phi\left(f_2\right) \right\} \tag{9}$$

The model to calculate thermal conductivity is developed by averaging the multiple values of the constituents that directly make up the composite material. Therefore, when we average the two possible cases we can have the thermal conductivity of the three-phase mixture [19] as

$$k = \frac{k_0}{2}\left\{ \Psi\left[\frac{f_1}{(1-f_2)}\right]\Phi\left(f_2\right) + \Phi\left[\frac{f_2}{(1-f_1)}\right]\Psi\left(f_1\right) \right\} \tag{10}$$

where k_0 is the thermal conductivity of the matrix, $\Psi\left(f\right)$ and $\Phi\left(f\right)$ are functions describing the effect of defects on the thermal conductivity of the coating. This process is also known as an averaging technique. This process of averaging the all possible ways in which different types of defects can be added will provide the formula for n number of defects under consideration. A five-phase model will have 24 different equations that will be averaged to obtain thermal conductivity of coating. Therefore, for the five-phase model, there are four different types of defects that are assumed to be embedded in a continuous matrix.

C. Five-phase model

The volumetric fractions of different types of defects are given by f_1, f_2, f_3 and f_4. The effect of each defect on thermal conductivity is given by functions $\Phi(f)$, $\Psi(f)$, $\Theta(f)$ and $\beta(f)$, respectively. The values of volumetric fraction are obtained from image analysis using Image J and from references using MIP (Mercury Intrusion Porosimetry). The functions are all defined by the equation (6). The five-phase model can be expressed as

$$k = \frac{k_0}{24}\left(A+B+C+D\right) \tag{11}$$

where A, B, C and D provides simplification of the formula. The formula averages all the possible conditions in which the four different types of defects can be added in different sequences. The details regarding the A, B, C and D can be found somewhere else [23].

IV. DATA RESOURCES

The data for the modelling work is obtained from several references, Image analysis and from MIP. The image analysis and MIP provide the details regarding the volumetric fraction of various kinds of defects present in the coating. In this work, a spheroidal shape is used to model various kinds of defects. This shape can cover a large number of real-life defects that are present in the coating.

Image J provides the details regarding the porosity content present in the coatings. The four types of defects that are under consideration are open randomly oriented cracks, microcracks, non-flat spheroids porosity and defects having revolution axis oriented perpendicular to heat flux (penny-shaped defects). The equation (6) is used to define the functions and equation (7) is used to obtain the values of X. The X-factors obtained during this study are listed below in Table 1. Overall porosity content can be seen in Table 2 that are obtained from image analysis.

Table 1 X factor for different defects [23]

X-Factor	Functions
1.66	Open Randomly Oriented
7	Microcracks
2	Penny shaped (α=90°)
1.7	Non-flat porosity

Table 2 Overall Porosity Content of various coatings

Coatings	Overall Porosity (%)
8YSZ (As-sprayed)	24.5
8YSZ (Annealed)	20.7
22MSZ (As-sprayed)	18.9
22MSZ (Annealed)	16.8
25CSZ (As-sprayed)	23.7
25CSZ (Annealed)	13.9
F&C (As-sprayed)	21.3
F&C (Annealed)	16.9
A&S (As-sprayed)	17.9
A&S (Annealed)	16.1
HOSP (As-sprayed)	19
HOSP (Annealed)	14.4

V. RESULT AND DISCUSSION

A. Obtained Thermal Conductivity

The five-phase model is used to calculate the thermal conductivity of the coating using the porosity content, volumetric fraction and the X values. The values of thermal conductivity for various coatings can be obtained from Table 3.

Table 3 Thermal conductivity values obtained using five-phase model

Coatings	Thermal Conductivity (W/mK)
8YSZ (As-sprayed)	1.18
8YSZ (Annealed)	1.60
22MSZ (As-sprayed)	1.14
22MSZ (Annealed)	1.35
25CSZ (As-sprayed)	1.175
25CSZ (Annealed)	1.93
F&C (As-sprayed)	1.2
F&C (Annealed)	1.79
A&S (As-sprayed)	1.33
A&S (Annealed)	1.56
HOSP (As-sprayed)	1.12
HOSP (Annealed)	1.36

B. Validation of Results

The results obtained from the five-phase model are validated against experimental results. Thermal conductivity of different coatings obtained from the five-phase model, four-phase model and experimental results are compared in Figure 2. Thermal conductivity values of different Yttria Stabilized Zirconia (YSZ) obtained from the five-phase model, experimental and FEA model are compared in Figure 3.

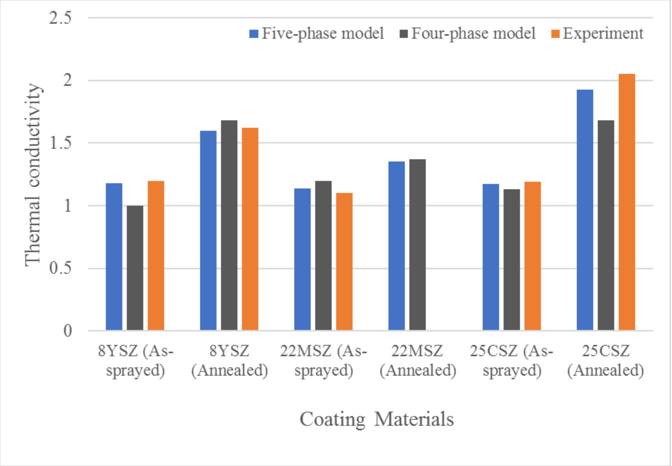

Figure 2 Comparison of thermal conductivity values.

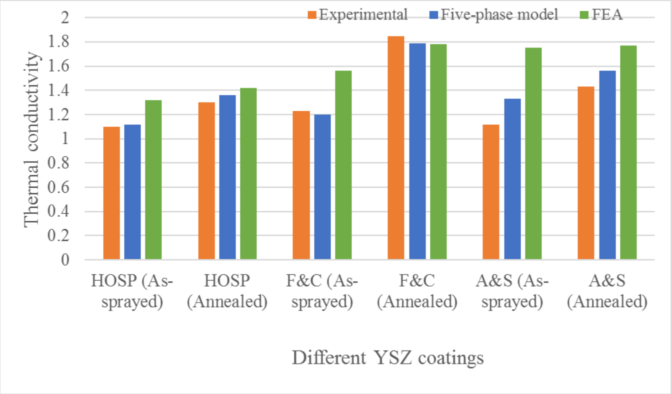

Figure 3 Comparison of thermal conductivity values for various YSZ coatings

VI. CONCLUSION

A five-phase model to predict thermal conductivity of thermal barrier coatings was developed in this work and validated against the results from the four-phase model, FEA model and experimental results. The presented model takes into consideration the different types of pores that are mostly present in a topcoat. The parameters used in the model were obtained from previous models and fitting parameters. The results obtained with the new proposed model were then validated against the reference data.

By comparing the predicted values with experimental results, it was shown that the proposed five-phase model can predict the thermal conductivity of ceramic coatings closer to the actual values. The five-phase model can predict the values of thermal conductivity within 6% of the experimental results. The proposed model uses real microstructure images and MIP results to obtain porosity content in the coatings to better predict the thermal conductivity. The proposed model has the potential to predict microstructure-property relationships.

The presence of different types of pores and cracks influences the overall thermal conductivity of the coatings. Microcracks present in the coating's microstructure influence the thermal conductivity. The density of microcracks is affected by heat treatment due to the expansion of the coating material. Smaller cracks disappear in the coating due to sintering and lead to lower porosity content, which ultimately leads to an increase in thermal conductivity.

ACKNOWLEDGEMENT

This research is supported by the Air Defence System Program of the National Research Council Canada and the Natural Sciences and Engineering Research Council of Canada.

REFERENCES

[1] R. C. Reed, *The Superalloys: Fundamentals and Applications by Roger C. Reed*. Cambridge University Press, 1742.

[2] A. K. Ray and R. W. Steinbrech, "Crack propagation studies of thermal barrier coatings under bending," *J. Eur. Ceram. Soc.*, vol. 19, no. 12, pp. 2097–2109, Oct. 1999.

[3] W. J. Brindley and R. A. Miller, "Thermal barrier coating life and isothermal oxidation of low-pressure plasma-sprayed bond coat alloys," *Surf. Coat. Technol.*, vol. 43–44, no. 1–3, pp. 446–457, 1990.

[4] K. Kokini and Y. R. Takeuchi, "Initiation of surface cracks in multilayer ceramic thermal barrier coatings under thermal loads," *Mater. Sci. Eng. A*, vol. 189, no. 1, pp. 301–309, Dec. 1994.

[5] J. R. Brandon and R. Taylor, "Thermal properties of ceria and yttria partially stabilized zirconia thermal barrier coatings," *Surf. Coat. Technol.*, vol. 39–40, pp. 143–151, 1989.

[6] A. Vardelle *et al.*, "The 2016 Thermal Spray Roadmap," *J. Therm. Spray Technol.*, vol. 25, no. 8, pp. 1376–1440, Dec. 2016.

[7] A. Fahr, B. Rogé, and J. Thornton, "Detection of thermally grown oxides in thermal barrier coatings by nondestructive evaluation," *J. Therm. Spray Technol.*, vol. 15, no. 1, pp. 46–52, Mar. 2006.

[8] H. M. Tawancy, A. I. Mohammad, L. M. Al-Hadhrami, H. Dafalla, and F. K. Alyousf, "On the performance and failure mechanism of thermal barrier coating systems used in gas turbine blade applications: Influence of bond coat/superalloy combination," *Eng. Fail. Anal.*, vol. 57, pp. 1–20, Nov. 2015.

[9] R. A. Miller, "Thermal barrier coatings for aircraft engines: history and directions," *J. Therm. Spray Technol.*, vol. 6, no. 1, p. 35, Mar. 1997.

[10] X. F. Zhang *et al.*, "Enhanced properties of Al-modified EB-PVD 7YSZ thermal barrier coatings," *Ceram. Int.*, vol. 42, no. 12, pp. 13969–13975, 2016.

[11] L. Wang *et al.*, "Influence of pores on the thermal insulation behavior of thermal barrier coatings prepared by atmospheric plasma spray," *Mater. Des.*, vol. 32, no. 1, pp. 36–47, 2011.

[12] J. Zhang and V. Desai, "Evaluation of thickness, porosity and pore shape of plasma sprayed TBC by electrochemical impedance spectroscopy," *Surf. Coat. Technol.*, vol. 190, no. 1, pp. 98–109, 2005.

[13] J. Wang *et al.*, "Effect of spraying power on microstructure and property of nanostructured YSZ thermal barrier coatings," *J. Alloys Compd.*, vol. 730, no. Supplement C, pp. 471–482, Jan. 2018.

[14] G.-R. Li, G.-J. Yang, C.-X. Li, and C.-J. Li, "A comprehensive mechanism for the sintering of plasma-sprayed nanostructured thermal barrier coatings," *Ceram. Int.*, vol. 43, no. 13, pp. 9600–9615, Sep. 2017.

[15] L. Liu, H. Zhang, X. Lei, and Y. Zheng, "Dependence of microstructure and thermal conductivity of EB-PVD thermal barrier coatings on the substrate rotation speed," *Phys. Procedia*, vol. 18, no. Complete, pp. 206–210, 2011.

[16] D. A. G. Bruggeman, "Berechnung verschiedener physikalischer Konstanten von heterogenen Substanzen. I. Dielektrizitätskonstanten und Leitfähigkeiten der Mischkörper aus isotropen Substanzen," *Ann. Phys.*, vol. 416, pp. 636–664, 1935.

[17] S. Banisi, J. A. Finch, and A. R. Laplante, "Electrical conductivity of dispersions: A review," *Miner. Eng.*, vol. 6, no. 4, pp. 369–385, Apr. 1993.

[18] D. R. Clarke, M. Oechsner, and N. P. Padture, "Thermal-barrier coatings for more efficient gas-turbine engines," *MRS Bull.*, vol. 37, no. 10, pp. 891–898, Oct. 2012.

[19] F. Cernuschi, S. Ahmaniemi, P. Vuoristo, and T. Mäntylä, "Modelling of thermal conductivity of porous materials: application to thick thermal barrier coatings," *J. Eur. Ceram. Soc.*, vol. 24, no. 9, pp. 2657–2667, Aug. 2004.

[20] Z. Wang, A. Kulkarni, S. Deshpande, T. Nakamura, and H. Herman, "Effects of pores and interfaces on effective properties of plasma sprayed zirconia coatings," *Acta Mater.*, vol. 51, no. 18, pp. 5319–5334, Oct. 2003.

[21] S. Wei, W. Fu-chi, F. Qun-Bo, and M. Zhuang, "Effects of defects on the effective thermal conductivity of thermal barrier coatings," *Appl. Math. Model.*, vol. 36, no. 5, pp. 1995–2002, May 2012.

[22] M. Zhao, W. Pan, C. Wan, Z. Qu, Z. Li, and J. Yang, "Defect engineering in development of low thermal conductivity materials: A review," *J. Eur. Ceram. Soc.*, vol. 37, no. 1, pp. 1–13, Jan. 2017.

[23] R. S. Ghai, "Modelling Thermal Conductivity of Porous Thermal Barrier Coatings for High-Temperature Aero Engines," Thesis, Université d'Ottawa / University of Ottawa, 2017.